



Discussion

Filament-induced amplified spontaneous emission in air–hydrocarbons gas mixture



Sima Hosseini^{*}, Ali Azarm, Jean-François Daigle, Yousef Kamali¹, See Leang Chin

Department of Physics, Engineering Physics and Optics & Center for Optics, Photonics and Laser (COPL), Université Laval, Québec City, QC, Canada G1V 0A6

ARTICLE INFO

Article history:

Received 15 August 2013

Received in revised form

14 October 2013

Accepted 11 November 2013

Available online 28 November 2013

Keywords:

Filament

Amplified spontaneous emission (ASE)

Fluorescence

ABSTRACT

Filament-induced amplified spontaneous emission, ASE, in air–hydrocarbons ($\sim 2\%$) gas mixture, CH_4 , C_2H_2 , and C_2H_4 , was investigated by detecting fluorescence emitted from CH fragments prepared in the electronically excited $\text{A}^2\Delta$ state in the filament. The fluorescence signal recorded from the side direction of the filament was linearly proportional to the length of the filament, while the fluorescence signal emitted in the backward direction of the laser propagation increased nonlinearly with the filament length. This difference showing that the filament acted as a gain medium in which the spontaneous emission from CH was amplified (ASE). This process realized by a small amount of hydrocarbon molecular species in air can be applied to remote sensing of pollutants in air.

© 2013 Elsevier B.V. All rights reserved.

1. Introduction

Intense femtosecond laser pulse propagation in air shows a unique property which is called filamentation. Filament in air results from a dynamic interplay between self-focusing induced by the neutral air molecules and defocusing from the plasma produced via multiphoton/tunnel ionization of air molecules [1–7]. In recent years, filamentation has been regarded as one of the most attractive phenomena induced by femtosecond laser propagation not only by its complex and characteristic mechanisms leading to intensity clamping [8–10] and lasing action in air [11–15] but also by a variety of its applications such as lightning triggering [16–18], remote sensing [19,20], THz generation [21] and ‘rain’ making [22] etc.

It was recently demonstrated that many kinds of chemical species in air existing as pollutants can be detected and identified by observing the backward fluorescence from the filament produced in air [5,19,20]. Indeed, through the recent investigations by filament-induced fluorescence spectroscopy, lasing action occurring in the filament [11,12] could enhance the sensitivity of the detection of pollutants in air in atmospheric remote sensing.

The importance of this phenomenon (lasing action in filament) aroused some new work on this subject. The lasing action along the laser propagation direction, that is, in the forward direction, was observed by Yao et al. [13], who generated amplified high-order harmonics in the filaments in air using near-infrared light.

On the other hand the lasing action along the direction opposite to the laser propagation direction, that is, along the backward direction, was observed by Dogariu et al. [14], who sent ultraviolet (226 nm) laser pulses through air. Also, high-energy backward lasing (with the energy of up to 300 nJ) in the atmosphere has been implemented by Traverso et al. [23]. Lasing generation in molecular nitrogen in an argon–nitrogen gas mixture in a femtosecond laser filament was observed by Kartashov et al. [24]. They showed that a mid-infrared wavelength filament-assisted nitrogen laser can be at least as efficient as its conventional discharge-pumped counterpart. In a theoretical investigation [25], the backward lasing action of N_2 and O_2 in air through the igniter–heater technique was proposed. Essentially, the intense femtosecond laser pulse (the igniter) creates a lasing-filament in air while liberating some seed electrons. A second, longer pulse (the heater) accelerates the seed electrons and initiates an electron avalanche resulting in more gain. This technique would result in the generation of a strong, coherent, counter-propagating optical pulse which provides a tool for various remote-sensing applications [25].

In the present study, we report the experimental results on the Amplified Spontaneous Emission induced by filament in air–hydrocarbons ($\sim 2\%$) gas mixture, CH_4 , C_2H_2 , and C_2H_4 . By comparing the fluorescence signal of the $\text{A}^2\Delta$ – $\text{X}^2\Pi$ emission band of CH radicals emitted in the direction perpendicular to the laser propagating direction, hereafter called the side direction, and that emitted in the backward direction, it was confirmed that amplification process originated from the electronically excited states of CH was created in the filament in air contaminated with a low percentage of hydrocarbon molecular species. Therefore, the idea of lasing action even in such a low percentage of air pollutant is clearly confirmed.

^{*} Corresponding author. Tel.: +1 418 614 9677.

E-mail address: sima.hosseini.1@ulaval.ca (S. Hosseini).

¹ Present address: Department of Physics, Faculty of Science, University of Mohaghegh Ardabili, PO Box 179, Ardabil, Iran.

2. Experiment

Using a mode-locked Ti:Sapphire chirped pulse amplification (CPA) system operating at 10 Hz repetition rate, we generated transform limited pulses with a width of 58 fs FWHM (full width at half-maximum), a central wavelength at 800 nm, and a maximum pulse energy of 12 mJ/pulse after a portable compressor. In the two-pass amplifier (inside CPA system), a half-wave plate and a polarizer, installed before the gain medium, were used to change the output energy.

The schematic diagram of the experimental setup used to record the fluorescence emitted in the side direction is shown in Fig. 1 and that used to record the fluorescence emitted in the backward direction is shown in Fig. 2. In both cases, the laser beam was focused by a plano-convex lens (L3, $f=1000$ mm) into a tube filled with a gas mixture, air with 2.0% hydrocarbon molecular species, whose total pressure was 1 atm.

In order to record an image of the filament (to measure the filament's length) as well as fluorescence signal from the side direction, the fluorescence emitted from the whole filament zone was projected through a periscope, two metallic mirrors and two fused silica lenses, onto the entrance slit (2 mm width) of a spectrometer (Acton Research Corporation, Spectra Pro 500i) equipped with an intensified charged-coupled device (ICCD) camera (Princeton Instruments, PIMAX 512) as shown in Fig. 1. For recording the image of the filament, the zero-th order reflection of the grating (1200 groove/mm) was used. In recording a spectrum using the first-order reflection of the grating, the wavelength resolution of 0.3 nm was achieved when the slit width was 100 μm . The ICCD detector was operated in the gating mode that transmitted mostly the molecular fluorescence into the detector so as to minimize the background light.

Since the length of the filament generated by the output beam of the compressor was longer than the opening of the side window, a telescope was used to increase the beam diameter. By this way we reached to the filament lengths shorter than the opening of the side window which made it possible to collect all of

fluorescence signal in the side direction. Besides that, in the current experiment for all different mixture of hydrocarbons and air, the results were achieved in single filament regime. Thus experiment was done in a special range of the pump power to prevent the beam from breaking up to several numbers of filaments (multiple filaments regime). Although more amplification of spontaneous emission would have been achieved by the longer filament, these two factors (diameter of the side window and formation of multiple filaments) restricted us to reach to longer filament length.

The backward fluorescence was collected with the fused silica lens (L4 in Fig. 2), whose focal length is $f(L4)=200$ mm onto the entrance end of a 3 m long fibre bundle (Princeton Instruments, Model LG-455-020), and was guided to the entrance slit of the spectrometer through an Imaging Fiber Adaptor (IFA in Fig. 2). In addition, an interference filter that transmits 431 nm light with the spectral bandwidth of 2.5 nm (FWHM) is placed in front of the fiber head to avoid introducing the strong white light into the fiber.

The sample gas tube was first evacuated to a background pressure of 4×10^{-2} Torr, and then, the air (98%) and hydrocarbon (2%) were mixed in the gas tube so that the total pressure became 760 Torr. The concentration of 2% was chosen because the lower flammable limits of the CH_4 , C_2H_2 , and C_2H_4 in air are 4.4%, 2.5% and 2.7%, respectively [26].

3. Results and discussion

In Fig. 3, we show the spectrum of the filament-induced fluorescence of air (black) and that of air–acetylene (2%) gas mixture (red) which was recorded from the side. The fluorescence spectra for the mixture of air with ethylene and air with methane were found to be almost the same as the one for the mixture of air with acetylene. The fluorescence signal appearing at around 431 nm corresponds to the $\text{A}^2\Delta\text{--X}^2\Pi$ (0,0) transition of CH fragments [27]. The origin of each fluorescence signal was the subject of many investigations. The fluorescence mechanism of hydrocarbons and nitrogen in strong laser field were discussed in [28–30]. The fluorescence mechanism in hydrocarbon was described as a neutral dissociation through superexcited states [28]. First, highly neutral excited states above the ionization potential, superexcited states, were populated through multiphoton excitation. Then the superexcited states could decay into different channels.

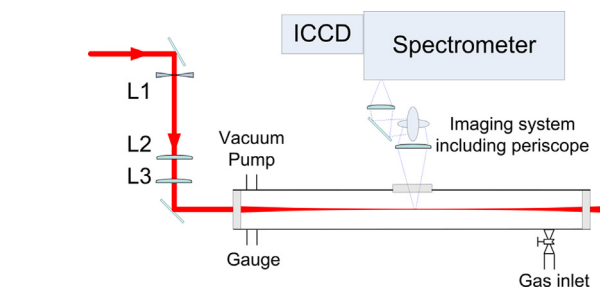


Fig. 1. Experimental setup for recording the image of the laser-induced filament as well as the side fluorescence intensity. The focal lengths of the two plano-convex lenses (L2 and L3) are +1000 mm and the focal length of the plano-concave lens (L1) is –200 or –250 mm.

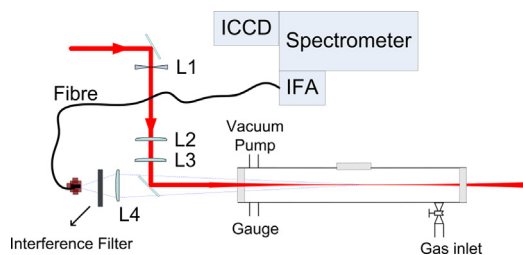


Fig. 2. Experimental setup for recording the backward fluorescence of the laser induced filament. The specifications of the optical components L1–L3 are the same as in Fig. 1. IFA stands for the imaging fiber adaptor.

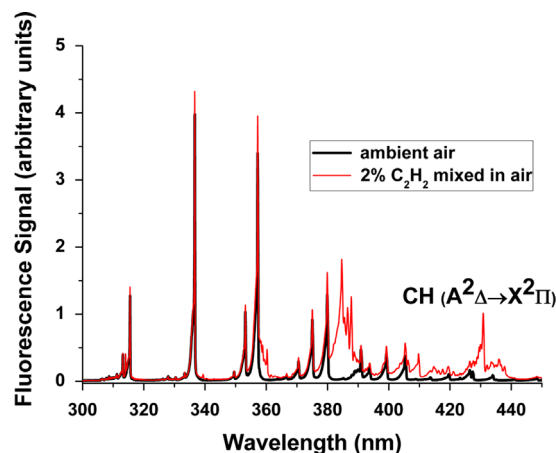


Fig. 3. The fluorescence emission spectrum from the laser-induced filament in ambient air (black) and that from the laser-induced filament in 2% acetylene in air (red). The $\text{A}^2\Delta\text{--X}^2\Pi$ (0,0) transition of CH fragments can be seen at around 431 nm. More precise spectroscopic assignments of the emission spectrum in the wavelength region above can be found in Refs. [28,29]. (For interpretation of the references to color in this figure legend, the reader is referred to the web version of this article.)

One of them is neutral dissociation. The lifetime of the super-excited state was measured for methane in a pump and probe experiment to be about 160 fs [31]. The CH ($A^2\Delta$) fragment created in a strong laser field decays to CH ($X^2\Pi$) resulting in the fluorescence signal at around 431 nm. Therefore the population inversion obtained by direct laser excitation through superexcited states.

Fig. 4 shows the observed filament images for the gas mixture of C_2H_4 (2%) in air recorded from the direction perpendicular to the light propagating axis, that is, the image of the side fluorescence, at four different input laser pulse energies. The length of the filament increases as the input laser pulse energy increases. In order to define the length of the filament, the recorded filament image (Fig. 4) was integrated along the direction perpendicular to the laser propagation direction to construct the averaged intensity distribution along the laser propagation direction. This integration was done for each gas mixture at different input energies. In the present study, the full width at half-maximum of the intensity distribution is defined as the effective length of the filament.

In this experiment, the white light continuum was found in the backward fluorescence but not from the side. In order to remove the contribution of the white light continuum, the emission spectrum between 429 and 432 nm, where the rotational band structure of the $A^2\Delta-X^2\Pi$ (0,0) emission transition is observed, was recorded first with the sample gas (air with 2% hydrocarbon molecules) as shown in Fig. 5 for CH_4 , (squares), and then the emission spectrum of air with the same partial pressure (0.98 atm) as in the gas mixture was measured (stars). By subtracting the emission spectrum of air from that of the gas mixture, the contribution from the CH emission was extracted as shown in the same figure for CH_4 (triangles). In the discussion below, the fluorescence signal integrated over the entire range of the background-subtracted fluorescence spectrum between 429 and 432 nm is defined as the signal of the backward fluorescence. Moreover, to record the backward signal we eliminated the reflection of the output window of the gas cell by the ICCD detector in the gating mode.

In Figs. 6–8, the integrated signal of the CH fluorescence for the backward and side fluorescence emission are plotted as a function of the filament length for the gas mixture of 2% C_2H_2 , C_2H_4 and CH_4 , respectively. In these figures it is clearly shown that although the total signal for the side fluorescence is linearly proportional to the filament length, the fluorescence signal for the backward direction increases nonlinearly as the filament length increases.

Before we discuss these trends in more detail, we first mention that in the current experiment, the intensity clamping [8,9] in the interaction of femtosecond laser pulses with gases plays a critical role and it is interpreted as a very important factor to find the gain coefficient in filament zone as the pump power is increased. As it is mentioned before, formation of filament is a result of the balance between self-focusing and defocusing due to the plasma generated inside the filament. The generated electron density has a threshold which saturates self-focusing and limits the peak intensity inside the filament by defocusing the beam [2]. Also, this constant electron density above the critical power has been observed in helium [32] and it has been shown both experimentally and numerically that the plasma density of the single filament in air is only slightly dependent on the laser power [33]. Thus even by increasing the pump power (above critical power and before multiple filamentation) the intensity is clamped and the ionization degree to generate plasma does not go beyond few percent for a gas at atmospheric pressure [2]. Therefore with a good approximation we can consider all parameters which are function of the intensity and influence the population inversion, for instance multiphoton superexcitation, unchanged by

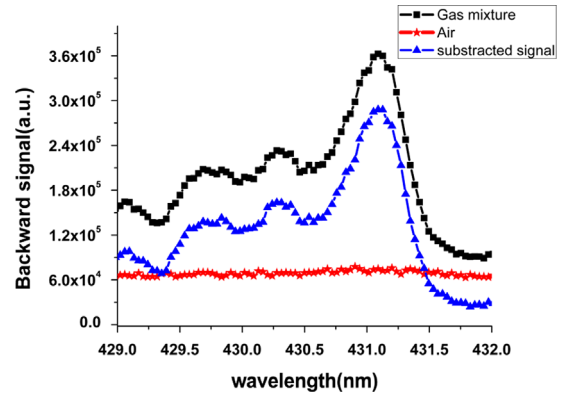


Fig. 5. The spectrum of the light emission from the laser-induced filament in 2% CH_4 mixed with air (squares), the spectrum of the background white light continuum in air (stars), and the difference spectrum (triangles) obtained by subtracting the white light continuum from the emission spectrum.

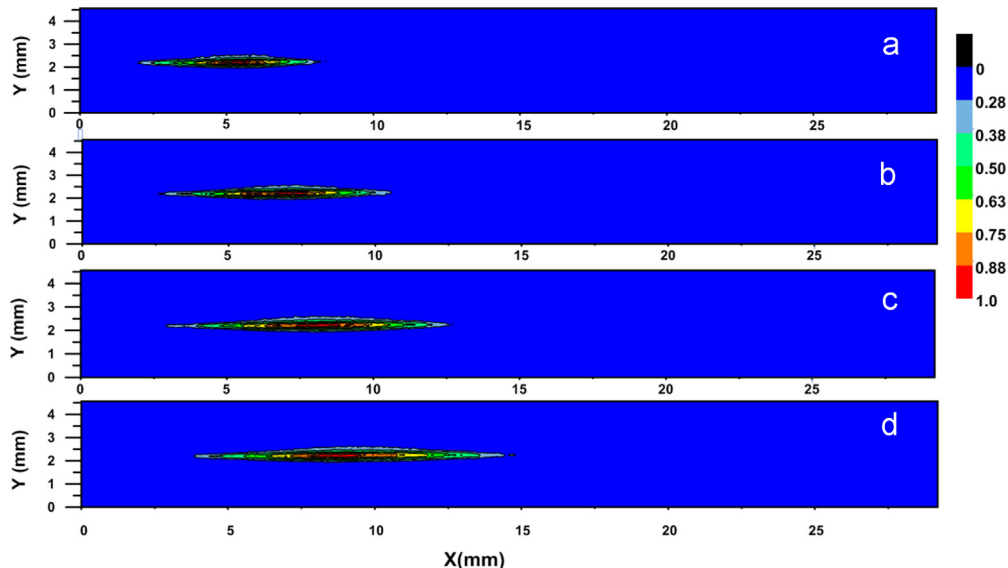


Fig. 4. The filament images of 2% C_2H_4 mixed in air. The pulse energies of the input pulses are 1.5, 2.5, 3.5, and 4.5 mJ/pulse in the descending order from (a) to (e). The laser beam propagates from right to left.

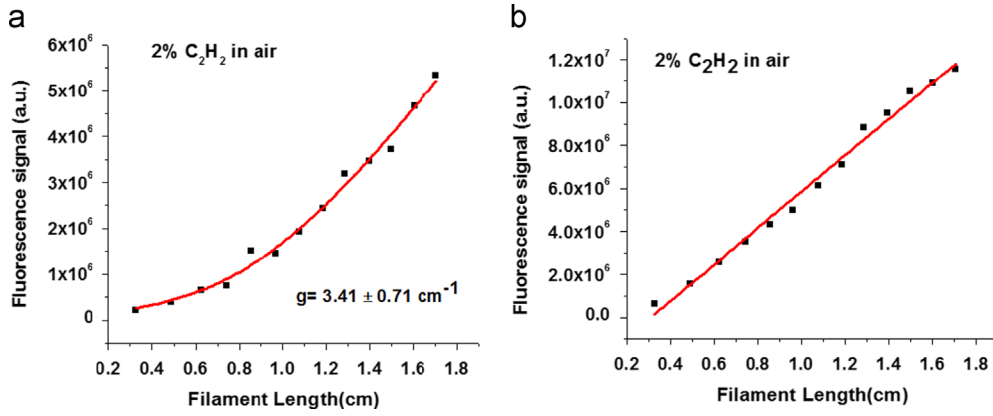


Fig. 6. The backward fluorescence (a) and the side fluorescence (b) emitted from the filament produced in air with 2% C_2H_2 mixed with air.

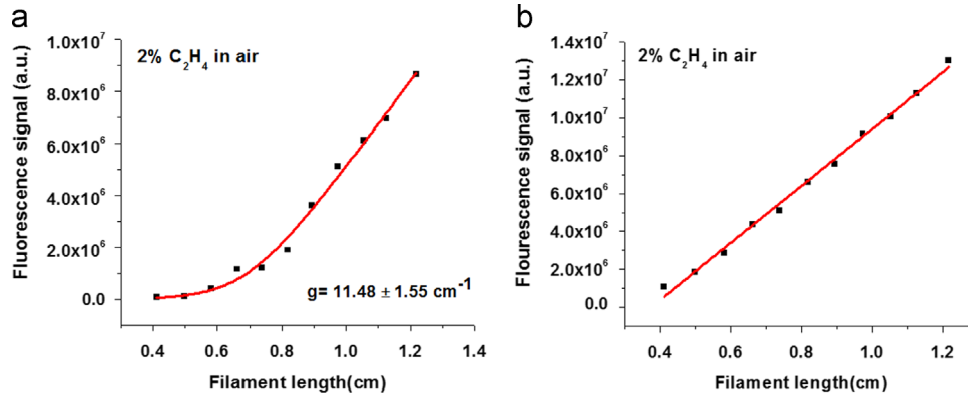


Fig. 7. The backward fluorescence (a) and the side fluorescence (b) emitted from the filament produced in air with 2% C_2H_4 mixed with air.

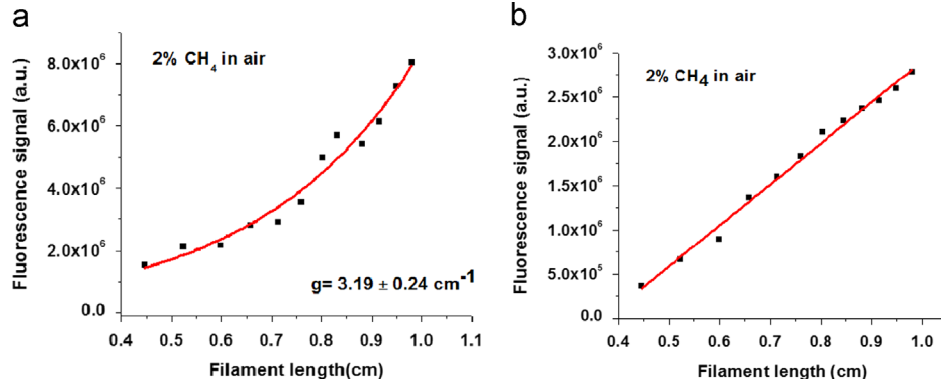


Fig. 8. The backward fluorescence (a) and the side fluorescence (b) emitted from the filament produced in air with 2% CH_4 mixed with air.

increasing the input power. So the gain would be considered same in single filament with different length and volume in different input power (above critical power and before multiple filaments form) since the intensity is clamped.

It is known that a gain medium can amplify the spontaneous radiation emitted by the excited molecules of the medium itself. A spontaneously emitted photon at one end of the amplifier can stimulate the emission of more photons and lead to substantial output radiation at the other end of the amplifier. This amplified emission regardless of whether there is any input radiation, is called ASE. If the amplification along a long thin cylindrical medium is sufficiently large, the output radiation can be quite bright, powerful and moderately directional [34–36]. Hence, such a medium emitting ASE is referred as mirror-less laser with output characteristics intermediate between a truly coherent laser oscillator and a completely incoherent thermal source [34–36]. As

reported previously in [11,12] the filament in air can act as a long and thin gain medium in which the ASE with high directionality is generated. In these primary experiments the condition of stationary population inversion was considered. In this work, we consider the more general condition by including the variation of the ASE intensity with space and time. The pump laser, which creates population inversion, is a pulse laser with femtosecond duration while ASE develops about a nanosecond later in the condition of the same time scale of decaying population inversion. Therefore time would play an important role in the calculation and explanation of the ASE results.

We notice that the filament length in this experiment was not more than 1.7 cm. This means that the femtosecond filamenting pulse took about 57 ps or less to go through the filament zone. However, the fluorescence lifetime of the excited species is of the order of a few nanosecond (ns). This is much longer than the

passage time, 57 ps or less, of the pump pulse. We thus can approximate that the initial population differences, N_0 , created by the pump pulse remains unchanged after the passage of the pump. Because of intensity clamping, we further approximate the filament zone as a narrow cylinder in which the initial population inversion is constant all over. The intensity of the ASE across the cross section of the cylinder is thus assumed uniform. We shall investigate whether this cylindrical medium can act as a gain system for contaminated air by hydrocarbon.

It is important to mention that because of the short duration of the pump pulse compared to the lifetime of the excited species, which is of the order of a few nanosecond (ns), the pumping process does not affect the level populations in the filament zone during the development of ASE. Thus the changes in population differences are mainly due to stimulated emission and spontaneous emission. So the rate equation for the population difference (N), considering an approximation which is explained in what follows, is

$$\frac{\partial N}{\partial t} = -\frac{2\sigma}{h\nu}NI \quad (1)$$

where σ is the cross section of stimulated emission and $h\nu$ is the photon energy. By considering the filament zone as an amplifier for spontaneous emission, we can write an equation for the variation of the intensity, I , in space and time:

$$\frac{\partial I}{\partial z} + \frac{1}{c} \frac{\partial I}{\partial t} = \sigma NI \quad (2)$$

where c is the speed of light. In Eqs. (1) and (2) we only consider the contribution of stimulated emission. But to calculate the ASE intensity, the elemental variation, dI , must account not only for the stimulated emission but also for the spontaneous emission. It is worth mentioning that there are two ways for the treatment of ASE. One way is adding a term to the right side of Eqs. (1) and (2) which is the contribution of spontaneous emission of photons. The other simplified way, is solving the ASE problem by considering an “effective noise input, I_{eff} ” [36]. This approach is based on Eqs. (1) and (2), which spontaneous emission term has been not considered in them. By integrating both sides of Eq. (2) over time and space then considering the solution of Eq. (1) for N , the following equation is obtained:

$$\varphi_{\text{out}} = A \ln [1 + e^{g\varphi} (e^{\varphi_{\text{eff}}/A} - 1)] \quad (3)$$

where $\varphi(z) \equiv \int_{-\infty}^{\infty} I(z, t) dt$, is the fluence which is a measure of the total energy content of the ASE. So $\varphi_{\text{out}} \equiv \varphi(L)$ represents the output fluence of the filament of length L and $\varphi_{\text{eff}} \equiv \varphi(0) = \int_{-\infty}^{\infty} I_{\text{eff}} dt$ gives the effective fluence of the gain medium. We note that this solution (Eq. (3)) gives $\varphi_{\text{out}} \equiv 0$ or $I(z, t) = 0$ for all z if $I(0, t) = 0$. Thus, some effective input $I(0, t) = I_{\text{eff}} \neq 0$ is necessary to take into account the spontaneous emission in order to obtain a non-vanishing $I(z, t)$. Also in this equation $A = h\nu/2\sigma$ and $g = \sigma N_0$ is the small signal gain coefficient where N_0 is the initial population differences at all z . As we explained already, because of the clamped intensity inside the filament we can take N_0 to be a constant in the integration over space in the narrow cylinder.

By using Eq. (3) we fitted a curve to the detected backward fluorescence signal as a function of the filament length (Figs. 6–8(a)). In the experiment, integrated fluorescence signal is a measure of fluence. The fitting parameters are g , φ_{eff} and A . By this fitting, $g = 3.41 \pm 0.71$, 11.48 ± 1.55 and $3.19 \pm 0.24 \text{ cm}^{-1}$ were obtained for the gas mixtures of 2% C_2H_2 , C_2H_4 , and CH_4 , respectively. From the side we observe a linear relation between the length of the filament and the total fluorescence signal (Figs. 6–8(b)).

To interpret these observations, it is important to mention that by increasing the laser power the diameter of filament increases as well as its length. Briefly, by increasing the initial laser power, more energy is injected into the filament volume defined as the high-intensity

volume where the clamping phenomenon maintains a maximum intensity. However, the defocusing due to the plasma generated inside the filament balances the self-focusing effect and leads to phenomena such as intensity clamping inside the filament (limited peak intensity) [8,9]. Therefore, an increase in filament's volume and cross sectional area with a clamped intensity has to occur, with the increase of the initial laser power before multiple filaments form as an effect of intensity clamping. As observed by others [9,37] the fluorescence signal is proportional to the filament's volume. Therefore the increase of the signal as a function of pulse energy (above critical power) is an indication of the growth of the filament volume, in which the intensity is clamped. The point is that the trend of changes in fluorescence signal as a result of increasing the volume should be same for all directions. But Figs. 6–8, clearly show that these trends are not same for back and side directions for all gas mixtures. This difference is due to the fact that on one hand the backward fluorescence signal is the amplified spontaneous emission signal and the filament zone acts as a gain medium for emission signal but on the other hand this kind of amplification is negligible from the side because of the very short diameter of the filament and it is covered by the effect of volume. Thus the origin of this difference in the results of back and side is the amplification of the signal which happened along the filament length. Otherwise other physical phenomena which may happen inside the filament by increasing the pump power would have the same effect on the trend of changes of emission signal for all directions. The collected fluorescence signal from the side in this experiment and comparing the result with backward fluorescence signal is an important evidence of existing amplification of emission along the filament length.

The observed gain shows that the population inversion is realized in CH. It is possible that hydrocarbon molecules are excited by multiphoton absorption of 800 nm light to their superexcited states, from which both the electronically excited CH in the $A^2\Delta$ state and the electronic ground $X^2\Pi$ state are created, and the population of CH in the electronically excited $A^2\Delta$ states becomes larger than that of CH in the electronic ground state. Even though the details of the mechanism of the formation of the superexcited states and their decay processes are not well-known, it is certain that 2% of hydrocarbon molecules in air can act as a gain medium when the filaments are generated by intense ultrashort laser pulses. Considering the gain in the CH fragments, measuring some characteristics of a medium such as population inversion ratio and molecular density of the medium are interesting physical issues to investigate in the future.

4. Conclusion

By focusing ultrashort laser pulses into the 2% mixtures of CH_4 , C_2H_2 and C_2H_4 in air at 1 atm, different trends of variation of fluorescence signal from CH fragments versus the length of filament were observed, from the back and the side. The results indicate the existence of ASE from the hydrocarbon molecules. For the description of ASE, we considered the non steady state equation for propagation of intensity in the amplifying medium (filament) characterized by a gain coefficient. It is expected that this amplified spontaneous emission process can be applied to remote sensing of pollutants in atmosphere with high sensitivity.

Acknowledgements

This work was partially supported by NSERC, Canada Research Chairs, FQRNT and CIPI. We appreciate the technical support and assistance of Mr. M. Martin at the Ultrafast Intense Laser Science

Laboratory, Université Laval, where the experiment was carried out. Also we appreciate very much the helps of Shigeki Owada, Atsushi Iwasaki and Prof. Kaoru Yamanouchi and their fruitful discussion in preparation of the paper.

References

- [1] S.L. Chin, S.A. Hosseini, W. Liu, Q. Luo, F. Theberge, N. Aközbek, A. Becker, V.P. Kandidov, O.G. Kosareva, H. Schroeder, *Can. J. Phys.* 83 (2005) 863.
- [2] A. Couairon, A. Mysyrowicz, *Phys. Rep.* 441 (2007) 47.
- [3] L. Bergé, S. Skupin, R. Nuter, J. Kasparian, J.-P. Wolf, *Rep. Prog. Phys.* 70 (2007) 1633.
- [4] V.P. Kandidov, S.A. Shlenov, O.G. Kosareva, *Quantum Electron.* 39 (2009) 205.
- [5] S.L. Chin, *Femtosecond Laser Filamentation*, Springer, 2010.
- [6] R.W. Boyd, S.G. Lukishova, Y.R. Shen (Eds.), *Self-Focusing: Past and Present Fundamentals and Prospects*, Springer, 2009.
- [7] J. Kasparian, J.-P. Wolf, *Opt. Express* 16 (2008) 466.
- [8] J. Kasparian, R. Sauerbrey, S.L. Chin, *Appl. Phys. B* 71 (2000) 877.
- [9] A. Becker, N. Aközbek, K. Vijayalakshmi, E. Oral, C.M. Bowden, S.L. Chin, *Appl. Phys. B* 73 (2001) 287.
- [10] W. Liu, S. Petit, A. Becker, N. Aközbek, C.M. Bowden, S.L. Chin, *Opt. Commun.* 202 (2002) 189.
- [11] Q. Luo, W. Liu, S.L. Chin, *Appl. Phys. B* 76 (2003) 337.
- [12] Q. Luo, A. Hosseini, W. Liu, S.L. Chin, *Opt. Photonics News* September (2004).
- [13] J. Yao, B. Zeng, H. Xu, G. Li, W. Chu, J. Ni, H. Zhang, S.L. Chin, Y. Cheng, Z. Xu, *Phys. Rev. A: At. Mol. Opt. Phys.* 84 (2011) 051802.
- [14] A. Dogariu, J.B. Michael, M.O. Scully, R.B. Miles, *Science* 331 (2011) 442.
- [15] S. Owada, A. Azarm, S. Hosseini, A. Iwasaki, S.L. Chin, K. Yamanouchi, *Chem. Phys. Lett.* 581 (2013) 21.
- [16] X.M. Zhao, J.-C. Diels, A. Braun, X. Liu, D. Du, G. Korn, G. Mourou, J.M. Elizondo, *Ultrafast phenomena*, Springer Series in Chemical Physics, P.F. Barbara, W.H. Knox, G.A. Mourou, A.H. Zewail (Eds.), Springer-Verlag, New York, 60 (1994) 233.
- [17] M. Rodriguez, R. Sauerbrey, H. Wille, L. Wöste, T. Fujii, Y.-B. André, A. Mysyrowicz, L. Klingbeil, K. Rethmeier, W. Kalkner, J. Kasparian, E. Salmon, J. Yu, J.-P. Wolf, *Opt. Lett.* 27 (2002) 772.
- [18] H. Pépin, D. Comtois, F. Vidal, C.Y. Chien, A. Desparois, T.W. Johnston, J.C. Kieffer, B. La Fontaine, F. Martin, F.A.M. Rizk, C. Potvin, P. Couture, H.P. Mercure, A. Bondiou-Clergerie, P. Lalande, I. Gallimberti, *Phys. Plasmas* 8 (2001) 2532.
- [19] H.-L. Xu, S.L. Chin, *Sensors* 11 (2011) 32.
- [20] S.L. Chin, H. Xu, Q. Luo, F. Théberge, W. Liu, J.-F. Daigle, Y. Kamali, P. Simard, J. Bernhardt, S. Hosseini, M. Sharifi, G. Méjean, A. Azarm, C. Marceau, O. Kosareva, V. Kandidov, N. Aközbek, A. Becker, G. Roy, P. Mathieu, J.-R. Simard, M. Châteauneuf, J. Dubois, *Appl. Phys. B* 95 (2009) 1.
- [21] C. D'Amico, A. Houard, M. Franco, B. Prade, A. Mysyrowicz, *Phys. Rev. Lett.* 98 (2007) 235002.
- [22] P. Rohwetter, J. Kasparian, K. Stelmaszczyk, Z. Hao, S. Henin, N. Lascoux, W.M. Nakaema, Y. Petit, R. Manuel Queiße, E. Salame, L. Salmon, Wöste J.P. Wolf, *Nat. Photonics* 4 (2010) 451.
- [23] A.J. Traverso, R. Sanchez-Gonzalez, L. Yuan, K. Wang, D.V. Voronine, A.M. Zeltikove, Y. Rostovtes, V.A. Sautenkov, A.V. Sokolov, S.W. North, M.O. Scully, *PNAS* 109 (2012) 15185.
- [24] D. Kartashov, S. Alisauskas, G. Andriukaitis, A. Pugzlys, M. Shneider, A. Zheltikov, S.L. Chin, A. Baltuska, *Phys. Rev. A: At. Mol. Opt. Phys.* 86 (2012) 033831.
- [25] P.R. Hemmer, R.B. Miles, P. Polynkin, T. Siebert, A.V. Sokolov, P. Sprangle, M.O. Scully, *PNAS* 108 (2011) 3130.
- [26] C.L. Yaws, W. Braker, *Matheson Gas Data Book*, seventh ed., McGraw Hill Professional, 2001.
- [27] R.W.B. Rears, A.G. Gaydon, *The Identification of Molecular Spectra*, fourth ed., Chapman and Hall Ltd, London, 1976.
- [28] F. Kong, Q. Luo, H. Xu, M. Sharifi, D. Song, S.L. Chin, *J. Chem. Phys.* 125 (2006) 133320.
- [29] A. Talebpour, M. Abdel-Fattah, A.D. Bandrauk, S.L. Chin, *Laser Phys.* 11 (2001) 68.
- [30] A. Azarm 2012 Ph.D., Dissertation Laval University.
- [31] A. Azarm, H.L. Xu, Y. Kamali, J. Bernhardt, D. Song, A. Xia, Y. Teranishi, S.H. Lin, F. Kong, S.L. Chin, *J. Phys. B: At. Mol. Opt. Phys.* 41 (2008) 225601.
- [32] J. Bernhardt, P.T. Simard, W. Liu, H. Xu, F. Théberge, A. Azarm, J.-F. Daigle, S.L. Chin, *Opt. Commun.* 281 (2008) 2248.
- [33] F. Théberge, W. Liu, P.T. Simard, A. Becker, S.L. Chin, *Phys. Rev. E: Stat. Nonlinear Soft Matter Phys.* 74 (2006) 036406.
- [34] A.E. Siegman, *Lasers*, University Science Books, 1986.
- [35] O. Svelto, *Principles of Lasers*, fifth ed., Springer, New York, 2009.
- [36] P.W. Milonni, J.H. Eberly, *Laser Physics*, Wiley, New Jersey, 2010.
- [37] E. Arevalo, A. Becker, *Phys. Rev. A: At. Mol. Opt. Phys.* 72 (2005) 043807.